Digital Communications and Networks 2 (2016) 196–205

HOSTED BY

ELSEVIER

Contents lists available at ScienceDirect

Digital Communications and Networks

journal homepage: www.elsevier.com/locate/dcan

Kernel fuzzy c-means clustering on energy detection based cooperative spectrum sensing☆

Anal Paul, Santi P. Maity*

Department of Information Technology,Indian Institute of Engineering Science and Technology, Shibpur, Howrah711 103, India[1]

ARTICLE INFO

Keywords:
Cooperative spectrum sensing
Kernel fuzzy c-means
Energy detection
Multiple PU detection

ABSTRACT

Cooperation in spectral sensing (SS) offers a fast and reliable detection of primary user (PU) transmission over a frequency spectrum at the expense of increased energy consumption. Since the fusion center (FC) has to handle a large set of data, a cluster based approach, specifically fuzzy c-means clustering (FCM), has been extensively used in energy detection based cooperative spectrum sensing (CSS). However, the performance of FCM degrades at low signal-to-noise ratios (SNR) and in the presence of multiple PUs as energy data patterns at the FC are often found to be non-spherical i.e. overlapping. To address the problem, this work explores the scope of kernel fuzzy c-means (KFCM) on energy detection based CSS through the projection of non-linear input data to a high dimensional feature space. Extensive simulation results are shown to highlight the improved detection of multiple PUs at low SNR with low energy consumption. An improvement in the detection probability by ~6.78% and ~6.96% at −15 dBW and −20 dBW, respectively, is achieved over the existing FCM method.

1. Introduction

The present wireless communication services work on the basis of static frequency spectrum allocation i.e. each service is assigned to a fixed frequency spectrum. This static allocation policy results in a spectrum under utilization state that in turn creates a spectrum scarcity problem due to the increased number of wireless devices with data intensive applications such as interactive and multimedia services [1,2]. The cognitive radio (CR) concept emerges as a potential solution to address this spectrum shortage problem [3]. In a cognitive radio network (CRN), the unlicensed users are known as secondary users (SU) or cognitive users (CUs) while the licensed users are known as primary users (PU). The part of the spectrum or the frequency band of the PU that remains idle or unused in a specific geographical area and at a particular time is termed as white space or a spectrum hole [4]. SUs are accorded opportunistic access of the available spectrum hole without creating any interference to the PUs. Therefore, CRs must have the PU's spectrum utilization information or detect the presence of the PUs transmission before starting its own transmission so as to avoid any interference to the PU. In other words, the CR has to dynamically detect the unused spectrum before the opportunistic use of those available spectrum [5]. Dynamic spectrum sensing (DSS), spectrum selection, dynamic spectrum allocation (DSA), and dynamic spectrum management framework (DSMF) are a few of the important and pivotal topics in the field of CR research [6].

Non-cooperative spectrum sensing (SS) (sensing by a single user without the exchange of multiple users' sensing information) is not often reliable enough due to several reasons, for example, the sensing time often is short in duration, sensing is done at a low signal-to-noise ratio (SNR), PU's signal attenuation, fading, shadowing, noise, receiver uncertainty, etc. [6–8]. Cooperative SS (CSS) that involves multiple SUs followed by some suitable fusion schemes has been studied extensively to improve sensing reliability [7,9,10]. Performance reliability of the SS is characterized by two probabilities. One of them is the probability of detection (P_d) that indicates the probability of correct detection of the PU transmission when the PU actually transmits over a frequency band. The other one is the probability of false alarm (P_{fa}) that represents the probability of presence of a PU transmission when it is not actually transmitting.

The literature on CSS is quite rich [11–19]. Different schemes, namely, energy detection (ED) [11,19], cyclostationary feature detection (CSFD) [12], eigenvalue based detection (EBD) [13], waveform based detection [14], matched filtering (MF) [15], generalized likelihood ratio test (GLRT) [16], wavelet based detection [18], and entropy based sensing [17] have been developed. The relative merits and demerits of each sensing scheme have also been reported in the

Peer review under responsibility of Chongqing University of Posts and Telecommunications.
* Corresponding author.
E-mail addresses: toanalpaul@gmail.com (A. Paul), santipmaity@it.iiests.ac.in (S.P. Maity).
[1] Formerly, Bengal Engineering and Science University, Shibpur, India.

http://dx.doi.org/10.1016/j.dcan.2016.09.002
Received 13 May 2016; Accepted 2 September 2016
Available online 17 September 2016

literature [20,21]. MF gives the optimal performance with high processing gain but it needs the knowledge of the PU signals, channel state information and synchronization among the receivers involved in the sensing process [22]. Waveform based detection shows fast sensing and higher accuracy in detection but requires a longer duration of a known sequence. This leads to lower efficiency of the spectrum utilization [21]. Eigenvalue based detection overcomes the noise uncertainty and sensing-receiver synchronization problem. However, it suffers from very complex computation and it requires larger sensing time compared to energy based detection [21]. Wavelet based detection has an ability to dynamically adapt with power spectral density (PSD) structures but it requires higher sampling rates for characterizing the complete spectrum bandwidth [21]. CSFD schemes show improved performance even at low SNR and can handle noise variance uncertainty [12]. However, drawbacks of the CSFD scheme are its very complex implementation, excessive computational cost and high power consumption [23,24]. CSFD gives poor sensing performance compared to ED [22], although ED is widely used due to its low computational complexity, low power consumption, very short sensing time and generic implementation [20]. More importantly, ED is found to be optimal in the absence of the knowledge of PU signal pattern [22]. However, ED suffers from noise uncertainty as well as uncertainty in the PU's signal covariance [25].

(A) *Machine Learning in CR works*: CR is a promising wireless transmission using autonomous learning about the other transmission to adapt to its dynamic environment [5]. The Machine Learning (ML) approach has been found to be effective in autonomous learning from the surroundings [26–30]. Application of ML in CR is substantially complicated due to several parameters and policies involved such as transmission power, channel coding and modulation scheme, SUs spatial diversities, spectrum sensing algorithm, fading, shadowing, communication protocol, sensing policy, noise uncertainties, security issues, etc. [27,28]. In spite of all these, ML is extensively applied in recent CR research for systematic adaption that does not need prior knowledge about the dependencies among the several parameters. In [31,32], the authors show that adaptive learning algorithms allow CUs to reconfigure the SS processes under various uncertainty conditions. In [33], the authors use a particle swarm optimization (PSO) and fast convergence PSO (FC-PSO) algorithms to address the sensing-throughput tradeoff under various SNR conditions. The authors in [28] proposed the CSS algorithm for CRN based on ML techniques such as unsupervised schemes like K-means clustering, Gaussian mixture model (GMM) and supervised schemes like support vector machine (SVM) and weighted K-nearest-neighbor (KNN) classification techniques. The methods reported are capable of implicitly learning the sensing environment and are found to be more adaptive than the traditional CSS hard fusion, e.g., OR/AND-rule-based and linear fusion [34,35]. Genetic algorithm (GA) based on ML approaches for improving optimization and performance results are reported in [36,37]. The authors in [38] proposed spectrum allocation methods based on GA, quantum genetic algorithm (QGA) and PSO. An intelligent cooperative spectrum sensing algorithm based on a non-parametric Bayesian learning model is reported in [30].

Several works are reported on energy efficient CSS [39,40]. It is well known that CSS improves sensing reliability at the cost of increased energy consummation due to the involvement of multiple nodes [40]. Energy consumption in CSS includes circuit power consumption and the energy requirement due to the transmission of sensing signal samples. Transmission energy consumption depends on several parameters, namely the number of SUs or relays involved, sensing duration i.e. number of samples needed and the associated power gain for the transmission of samples. Since circuit power consumption of the nodes for sensing PU signal is negligible compared to the amplifying gain, energy consumption largely depends on the relay power gain for transmission of sensing signals to the fusion center (FC). In other words, relay power gain was found to have a notable trade-off influence on sensing reliability and reduction in energy consumption [39]. Calculation of individual transmission power gains that involves multiple SUs is not always tractable. This is basically due to the lack of proper closed form mathematical expression. In [19], many parameters and a complex form of optimization are involved in simultaneous sensing of multiple channels to increase the channel capacity. Furthermore, computation complexity significantly increases with the number of relays [19,39]. Finding the solution using the numerous numerical computations involves a large number of parameters and demands a high computational cost and increased energy consumption [33,36–38,41]. Sometimes algorithms suffer from stuck to the local optimal values [32]. A low cost, tractable yet sub-optimal solution at low SNR may be a preferable choice. Cluster based approaches are found to be efficient to provide such solutions [40,42–44]. It is worth mentioning that cluster based approaches are efficiently used in medical image processing, bioinformatics, machine learning, information retrieval, data mining, statistical data analysis and in other problems [45–47].

(B) *Cluster Based approaches in CSS*: The literature on cluster based approaches in CR research are quite rich at this time [48,49,42,43,40,44]. Recent survey works on cluster-based SS in CRN are reported in [50,51]. In [48], the authors proposed a cluster based approach to decrease the number of sensing bits in SS. In [49], a multiple hop cluster based CSS scheme was proposed to reduce the power consumption. In [42], a cluster based approach was reported to reduce the effect of imperfect reporting channels on correlated log-normal shadow-fading channels. Work using clustering was proposed in [43] for improving cooperation among the secondary devices (users) that organize themselves in clusters according to both SS reliability and mobility behavior of each SEW. Fuzzy c-means (FCM) [40] and optimal FCM clustering [44] for ED based CSS are reported. Energy values of the PU signal received by multiple SOs are transmitted to the FC and using a selection combining scheme an energy data set is formed. FCM is then applied for the multiple-class clustering problem. On the other hand, differential evolution (DE) with FCM is used in [44] to separately address the problems of (i) maximizing the probability of detection under the constraint of the probability of a false alarm, (ii) SOs act as an amplify-forward (AF) relay and then minimization of the average energy consumption under the constraints of sensing reliability is done. Both the works partition the sensing energy into four classes, namely, strong presence, moderate presence, weak presence and absence of PU. SS reliability increases with the increase in the number of clusters. However, this performance gain is achieved at the expense of an increase in computation cost.

FCM has been found to be effective for spherical or linear data which means non-overlapping data inside the clusters. However, FCM performance deteriorates significantly when the data structure of the input patterns is non-spherical and complex [52]. At low SNR, the sensed data contains a lot of noise and the corresponding energy values become linearly inseparable in nature. In CSS, the sensed energy values that are particularly associated with the weak presence and the absence of the PU become inseparable. Projection of data (sensed energy) to a high dimensional space becomes essential for performance improvement in clustering. Kernel-fuzzy c-means (KFCM) maps nonlinear input data space into a high dimensional feature space. Projection to the higher dimensional space offers the scope of applying a linear classifier. Its application to the original input samples fails to reliably classify as the feature space could be extremely non-linear and inseparable [53]. Thus KFCM enables a mapping of the inseparable energy data sensed at a low SNR to a higher dimensional space where the data samples can more accurately be separated into the specific cluster. Though the direct computation in the high dimensional feature space consumes much time but Mercer kernels are used to make this practical [54]. This motivates us to use KFCM based clustering algorithm on CSS at a very low SNR. It was mentioned earlier that the increase in the cluster number [44] improves SS reliability but as the number of cluster increases the computational time and cost also increase. The computational complexity of KFCM and FCM was found to be the same [54]. Hence, reduction in the cluster numbers while maintaining the target sensitivity becomes a viable alternative and KFCM was found to be superior over FCM at low SNR.

(C) *Multiple PU detection*: Recent detection of multiple PUs in CSS becomes another challenge in CR research. However, works using SEW cluster based on multiple PU detection is not widely explored in the existing literature. A few notable works may be mentioned [55–58]. CSS, in the presence of multiple PUs, becomes difficult due to the involvement of several factors such as average distance between PU to SU, channel conditions, shadowing, PUs' transmit power, etc. [58]. SUs are assumed to be mostly battery powered, and need to be physically recharged or require battery replacement at regular time intervals. In the presence of multiple PUs in CRN, an energy effeciency and reliable SS can be implemented by associating a set of SUs to a particular PU signal sensing. A set of associated SUs, based on the sensing energy, forms a cluster. Hence, for N number of PUs in CRN, N number of SU clusters can be formed. An SU cluster-based CSS, for single PU detection, was reported in [10] where the authors suggested a cluster head for each cluster. In [55], the authors have done comparison of wide-band multiple PU detection using a weighted overlapped segment averaging (WOSA) approach. In [56,57], the authors addressed multiple PU detection using multiple antenna and a GLRT based approach. However, the above mentioned schemes [56,57] require excessive computational cost which leads to a greater energy consumption.

This work considers an ED based multiple PU detection scheme at low SNR using FCM and KFCM. A set of SOs forms a cluster to sense a particular PU signal using a probabilistic approach. The contributions of the present work are as follows:

- Partitioning of the inseparable energy data at low SNR into the respective clusters is done through the projection to a high dimension using KFCM. This results in an overall detection performance improvement over FCM [40,44].
- Detection of multiple PUs using ED based CSS by associating a particular set of SOs as a cluster to sense a particular PU.
- Extensive simulation results show improved detection performance at low energy consumption and at a smaller number of clusters (hence at reduced computation) over the existing FCM based method [40] and analytically approach [39].

Simulation results also show that the proposed KFCM based scheme requires reduced transmission energy values and offers faster sensing (less samples required) compared to the existing works while meeting the same detection reliability.

The article uses a large number of symbols which are included in Table 1. The remainder of the paper is organized as follows: the system model is presented in Section 2, while the proposed CSS algorithm is discussed in Section 3. Numerical results and analysis are demonstrated in Section 4. Finally, conclusions are highlighted in Section 5.

Table 1
List of symbols.

Symbol	Description
L	Number of unlicensed SUs/diversity number
T_{sense}	Spectrum sensing interval
t_s	Spectrum sensing slot
t_{s1}, t_{s2}	Spectrum sensing sub-slots
s_i	PU transmitted signal
P_p	PU transmission power
N	Number of PU samples
h_i	Channel gain between PU and respective SU
d_a	Distance between PU transmitter and SU
d_b	Distance between SU to FC
α	Path loss exponent
x_i	Received signal at SU_i during t_{s1}
η_i	SU_i receiver noise
P_n	Noise variance/power
E_{max}	Strongest measured signal energy at FC (using SC)
μ_{jz}	Membership value of each element in E_{max}
v_1, v_2, v_3, v_4	Set of cluster center
C_1, C_2, C_3, C_4	Set of cluster
P_d	Probability of detection
P_{fa}	Probability of false alarm
$\mathcal{P}(\mathcal{H}_1)$, $\mathcal{P}(\mathcal{H}_0)$	Probability of PU being active and idle
w_i	Individual SU amplifying gain
w_c	Total amplifying gain of all SUs
$w_{c_{ij}}$	Amplifying gain for the jth SU in the ith cluster
$d_{a_{ij}}$	Distance from a PU to the jth SU in the ith cluster
P_i	Average transmission power of SU_i
T_{sa}	Sampling interval
E_{BP}	Energy consumption in baseband processing circuits
E_{PA}	Energy consumption due to the amplification at SU
E_c	Energy consumption at radio devices during signal reception and transmission
E_s	Average energy consumption of all SUs

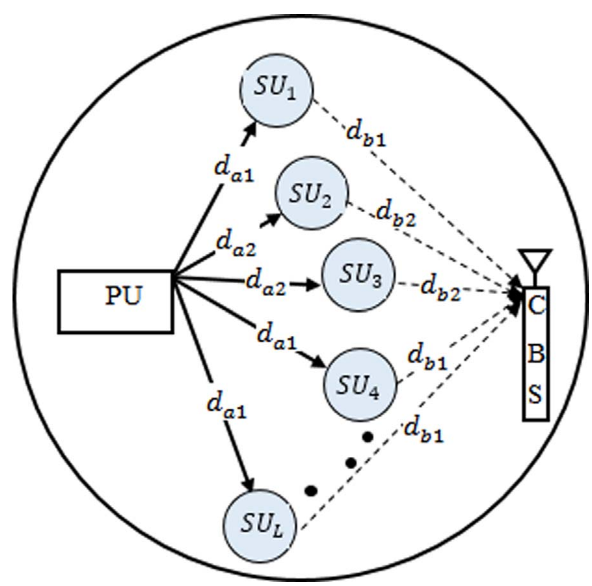

Fig. 1. Single *PU* system model.

2. System model

This section presents the proposed system model. The system model for CSS of a CRN with a single PU is shown in Fig. 1. The network consists of L number of SUs, which are indexed as (SU_1,SU_2,..SU_L), a PU and a cognitive base station (CBS) or FC. The FC contains multiple antennas that are represented as (AT_1,AT_2,..AT_L). CSS exploits spatial diversity of the SUs in the sense that SUs are assumed to be scattered about the area. However, truly scattered placement of the SUs needs channel adaptive unequal transmit power gain for the individual SU. A closed form solution to the individual SU transmit power gain is difficult to derive and computation complexity significantly increases with number of SUs [39]. The use of an optimal single power gain simplifies the analysis assuming that the SUs are co-located which is again unrealistic in practical situations. A viable alternative solution for an energy efficient system design may be a clustered based association where a set of SUs is assumed to be co-located and use a single transmit power [44]. In Fig. 1, for a single PU, SUs are assumed to be collocated in two different sets and form two clusters. The distance between the PU and SU_j is denoted by d_{a_j} and the same between FC and SU_j is denoted by d_{b_j}. The SUs, with the respective distances of d_{a_j} and d_{b_j}, form one cluster. Fig. 1 shows two such clusters of SUs for sensing a single PU. The PU's transmit power is represented by P_p. The sensing channels are considered to be Rayleigh

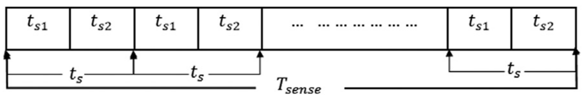

Fig. 2. Sensing time frame structure.

distributed and the reporting channels are considered to be ideal. The path loss exponent for the channel is denoted by α, which is distant dependent. The value of α is varied randomly and represents different channel conditions.

Fig. 2 represents the sensing frame structure. The sensing time interval (T_{sense}) is divided into multiple sensing slots, each one is denoted by t_s. Each individual t_s is again divided into two sub-slots, t_{s1} and t_{s2}. During the first sub-slot t_{s1} each *SU* receives a signal from the *PU*. In the next sub-slot t_{s2}, the *SU* forwards the sensed energy values to the FC. The FC has a selection combiner (SC) which selects the maximum energy signal among the received energy values. The selected energy values by the FC are stored as an energy set for further processing.

The symbol $x(t)$ indicates the received signal by a specific *SU* during t_{s1}. Hence, $x(t)$ is expressed as the sum of $s(t)$ and $\eta(t)$,

$$x(t) = s(t) + \eta(t) \tag{1}$$

where $s(t)$ is the PU signal and $\eta(t)$ represents the circularly symmetric complex Gaussian (CSCG) noise at the *SU* receiver. In CRN, the *PU*'s signal either appears to be present or absent in the received signal by the ith SU ($\forall\ i = 1, 2, 3\ldots.L$). Hence, detection of PU signal presence or absence leads to a binary hypothesis as follows:

$$\mathcal{H}_1\colon\ x_i(n) = h_i.\ s_i(n) + \eta_i(n) \qquad \forall\ n = 1, 2, 3\ldots.N \tag{2}$$

$$\mathcal{H}_0\colon\ x_i(n) = \eta_i(n) \qquad \forall\ n = 1, 2, 3\ldots.N \tag{3}$$

The symbol 'N' denotes the total number of observed PU samples during t_{s1}.

In Eq. (2), $h_i(n)$ represents the channel gain and is assumed to be $h_i(n) \sim CN(0, d_a^{-\alpha})$. The channel gain $h_i(n)$ depends on the distance (d_a) between the *PU* and the respective *SU*. The received signal energy depends on the *PU*'s transmit power, the SNR of the channel, noise variance and the path loss exponent(α). It is assumed that the PU signal $s_i(n)$ follows a circularly symmetric complex Gaussian (CSCG) distribution with zero mean and variance $E[|s_i(n)|^2] = P_p$. The noise $\eta_i(n)$ at SU_i is the independent and identically distributed (i.i.d) CSCG with zero mean and variance $E[|\eta_i(n)|^2] = P_n$. The energy for the received PU signal at SU_i is computed as $E_i = \sum_{n=1}^{N} |(x_i)|^2$. SU_i sends E_i to the FC during t_{s2}. The FC collects all the E_i values from L number of mutually independent SUs. Therefore the FC contains $E_{all} = \{E_i\}_{i=1}^{L}$. From this energy set ($E_{all}$), the FC selects the maximum energy value $\max\{E_{all}\}$ and stores E_{max} to form the energy data set for further processing. For different channel conditions the FC always stores the $\max\{E_{all}\}$ value in the E_{max} set.

The system model considered for multiple PU detection is shown in Fig. 3. It contains L number of SUs and multiple PUs. The distance between the SUs and PUs is different, indexed as $d_a = \{d_{a1}, d_{a2}, d_{a3}, d_{a4}, \ldots.., d_{aL}\}$. The distance from individual *SU* to the FC is also different and represented as $d_b = \{d_{b1}, d_{b2}, d_{b3}\ldots d_{bL}\}$. It is assumed that the PUs may have the same or different transmit power. It is assumed again that the path loss exponent(α) varies and indicates specific channel conditions. A set of SUs is assumed to sense a particular PU.

It is considered that all the SUs act as amplify-and-forward relays. It is assumed that the ith SU amplifies each received energy value by $\sqrt{w_i}$ and forwards the new energy value to the FC during t_{s2} [39]. w_i represents the power amplifying gain at the ith SU.

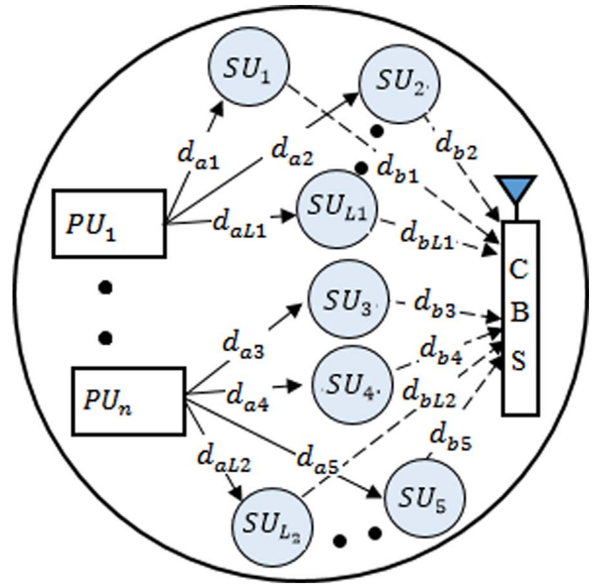

Fig. 3. Multiple *PU* system model.

3. Proposed KFCM based CSS method

This section focuses on improving the detection performance using KFCM over FCM. The working principle of FCM for CSS has been described in [40,44]. There are mainly two forms of KFCM. The first one comes from constructed prototypes in the feature space and is known as KFCM-F (F denotes feature space). The second one is KFCM-K, where the prototypes are preserved in the kernel space. In KFCM-K, there is an inverse mapping from the kernel space towards the feature space [54]. The KFCM-F technique is used in this work. The kernel-based method is performed on a random choice of non-linear mapping ϕ from the original d-dimensional feature space R^d to a higher dimension space. This is represented by the following Mercer kernel function (K_{ernel}):

$$K_{ernel}(x, y) \equiv \phi(x)^T\phi(y) \tag{4}$$

where $x, y \in R^d$. The distances are not computed in kernel space because it can be controlled by a Mercer kernel function. The Gaussian kernel function (GKF) is a type of Mercer kernel function. GKF makes the computation easy by transforming it into kernel space. GKF can be expressed as:

$$K_{ernel}(x, y) = e^{-\|x^2 - y^2\|/\sigma^2},\ \sigma^2 > 0 \tag{5}$$

where the symbol σ^2 represents the variance of GKF. Let us take a sample of the input data set $X = \{x_1, x_2, \ldots x_z\} \subseteq R^{Z\times d}$. Z is the number of samples in the input space. The symbol 'd' is the dimension of the sample x_z. KFCM minimizes the objective function as follows [54]:

$$Q = \sum_{j=1}^{J}\sum_{z=1}^{Z} \mu_{jz}^{m} \left\| \phi(x_z) - \phi(\nu_j) \right\|^2. \tag{6}$$

The symbol $m \in [1, \infty]$ is the fuzziness index. The symbol 'μ' is a partition matrix which contains the membership of x_z in the cluster v_j. x_z is the zth d-dimensional measured data, v_j is the d-dimension center of the jth cluster and ν_j ($j = 1, 2, 3, 4, \ldots.J$). The Euclidean distance $\|\phi(x_z) - \phi(\nu_j)\|$ is computed in the kernel space using the following equation:

$$\begin{aligned}\|\phi(x_z) - \phi(\nu_j)\|^2 &= \|\phi(x_z)^T\phi(x_z)\| + \|\phi(\nu_j)^T\phi(\nu_j)\| - 2\|\phi(x_z)^T\phi(\nu_j)\| \\ &= K_{ernel}(x_z, x_z) + K_{ernel}(\nu_j, \nu_j) - 2K_{ernel}(x_z, \nu_j).\end{aligned} \tag{7}$$

In the Gaussian kernel, $K_{ernel}(x_z, x_z) = 1$, finally

$$\|\phi(x_z) - \phi(\nu_j)\|^2 = 2(1 - K_{ernel}(x_z, \nu_j)). \quad (8)$$

The partition matrix μ and the updating of new cluster centers ν_j are optimized [54] as follows:

$$\mu_{jz} = \frac{1}{\sum_{i=1}^{J} \{1 - K_{ernel}(x_z, \nu_j)/1 - K_{ernel}(x_z, \nu_i)\}^{1/m-1}} \quad (9)$$

and

$$\nu_j = \frac{\sum_{z=1}^{Z} \mu_{jz}(K_{ernel}(x_z, \nu_i))x_z}{\sum_{z=1}^{Z} \mu_{jz}(K_{ernel}(x_z, \nu_i))}. \quad (10)$$

In the KFCM algorithm, the kernel matrix between the input data samples and the new cluster centers is computed during each iteration. The computational complexity for generating the partition matrix is $O(JZd)$, where 'J', 'Z' and 'd' are the number of clusters, the number of input samples and the dimension of the data, respectively. In other words, to find the new cluster center, the complexity is found to be $O(JZd)$. At each iteration, the kernel matrix requires JZ kernel function evaluations. This makes the total computational complexity $O(JZd)$ for KFCM-F, which is similar to the FCM time complexity [54]. The termination condition for both FCM and KFCM is

$$|\{present\}_{\mu_{jz}} - \{previous\}_{\mu_{jz}}| \le \epsilon$$

where ϵ is a threshold value, which represents the least difference between the present and the previous partition matrix 'μ'.

The maximum energy values are stored in E_{max} at the FC. This E_{max} is the input data space for both the clustering (FCM and KFCM) algorithms. E_{max} is partitioned into four clusters using the FCM algorithm [44,40]. In this proposed work, for low SNR, the E_{max} energy set is partitioned into three clusters using KFCM. The reason for a smaller number of clusters in KFCM is to maximize the inter-class distances. Four classes of FCM are denoted as strong presence (C_1), moderate presence (C_2), weak presence (C_3) and absence (C_4) of the PU signal. The FCM cluster centers are represented by $\{\nu_{j,1}, \nu_{j,2}, \nu_{j,3}, \nu_{j,4}\}$. Individual data, and each specific measured energy value ${E_{max}}^i$ (i.e. ith positions from E_{max}), are placed under one of these classes by comparing them with the cluster's center:

$$\min\{dist_{j,a} = |\nu_{j,a} - E_{max}^i|\}\begin{cases} \forall\ a = 1\ldots4 & \text{in } FCM \\ \forall\ a = 1\,..\,3 & \text{in } KFCM \end{cases} \quad (11)$$

Using FCM, the binary data patterns from C_1, C_2, C_3 are logically OR-ed to calculate P_d and P_{fa} depending on the hypothesis $\mathcal{H}_1$ and $\mathcal{H}_0$, respectively:

$$C_1 = \begin{cases} 1 & j,\ a^* = j,\ 1 \\ 0 & \text{otherwise} \end{cases},\quad C_2 = \begin{cases} 1 & j,\ a^* = j,\ 2 \\ 0 & \text{otherwise} \end{cases},\ C_3 = \begin{cases} 1 & j,\ a^* = j,\ 3 \\ 0 & \text{otherwise} \end{cases},$$
$$C_4 = \begin{cases} 1 & j,\ a^* = j,\ 4 \\ 0 & \text{otherwise} \end{cases}$$

In the present analysis, KFCM merges two clusters (strong presence and moderate presence) to a single cluster (strong presence). Hence, here KFCM considers three classes, namely, strong presence (C_1), weak presence (C_2) and absence (C_3) of the PU signal. It will be shown that three clusters based KFCM performs better in a low SNR energy data set due to transformation of the samples from input space to kernel space. Now three clusters based KFCM aims to maximize the inter-class distances and minimizes the intra-class distances among the data. The KFCM cluster centers are represented as $\{\nu_{j,1}, \nu_{j,2}$ and $\nu_{j,3}\}$. For KFCM, the binary data patterns of C_1,C_2 are logically OR-ed to calculate P_d, P_{fa}:

$$C_1 = \begin{cases} 1 & j,\ a^* = j,\ 1 \\ 0 & \text{otherwise} \end{cases},\quad C_2 = \begin{cases} 1 & j,\ a^* = j,\ 2 \\ 0 & \text{otherwise} \end{cases},\quad C_3 = \begin{cases} 1 & j,\ a^* = j,\ 3 \\ 0 & \text{otherwise} \end{cases}$$

3.1. Multiple PU detection

This subsection presents an energy based multiple PU detection scheme. Typically, the SU requires a particular antenna for the sensing of a particular PU signal. This means, if there is an N number of PUs in the CRN then each SU requires deploying N number of antenna. Each SU forwards the sensing energy of the individual PU to the FC, and transmission (SU to FC) of sensed samples requires a specific amount of energy consumption at the SU. It seems to be a multiple-input and multiple-output (MIMO) like architecture in CRN with complex implementation (multiple antennas in a SU) and heavy energy consumption at the SU due to the transmission of sensed samples to the FC. The proposed work helps to reduce the implementation complexity and energy consumption at the SU. During the initial sensing slot (learning stage), the SUs forward the sensing energy to the FC. For multiple PUs (PU_1,PU_2,..PU_n) in CRN, the FC stores the individual energy set for each PU such as $\{E_{maxPU1}, E_{maxPU2}, \ldots E_{maxPUn}\}$. In this proposed work, the FC divides the SUs into clusters using a probabilistic approach based on these energy sets. A set of associated SUs forms a cluster. Henceforth, an individual SU cluster senses a particular PU from the next sensing time slot. Each existing SU, in a specific cluster, is equipped with a single antenna instead of multiple antennas to sense a particular PU, which in turn reduces the overall implementation complexity. Furthermore, each SU of a particular cluster participates to sense a single PU, this means the SU needs to forward the sensed information of a particular PU to the FC. This in turn reduces the total energy consumption at the SU and improves the energy efficiency of the CRN.

The following example (Fig. 4) is used to describe the above issues. In this example, we consider the case with three SUs and two PUs in CRN. In the initial learning stage, all SUs participate in the sensing process of all the PU signals and forward the received signals to the FC. The FC stores E_{maxPU1} and E_{maxPU2} energy sets, respectively, for PU_1 and PU_2. The numerical values shown are the values of sensed energies in some unit.

From Fig. 4, the probability for the calculated E_{max} by SU_1 for the PU_1 as $E_{\max PU1}$ is denoted as $\mathcal{P}(SU_1) = 0.50$, and the same for SU_2 and SU_3 are $\mathcal{P}(SU_2) = 0.167$, $\mathcal{P}(SU_3) = 0.333$, respectively. From the E_{maxPU2} set, the probabilities are $\mathcal{P}(SU_1) = 0.333$, $\mathcal{P}(SU_2) = 0.50$ and $\mathcal{P}(SU_3) = 0.167$. The particular SU cluster is formed by comparing the individual SU's probability values for the different energy sets. In this example, there are two clusters formed as $SU_{c1} = \{SU_1, SU_3\}$ and $SU_{c2} = \{SU_2\}$. Hence SU_{c1} is allocated to sense PU_1, and SU_{c2} to PU_2 signal for the remaining sensing time slot.

3.2. Transmission energy calculations

The average transmission power of a specific SU_i is calculated as follows [44]:

$$P_i = (\mathcal{P}(\mathcal{H}_1)w_i((d_a)_i^{-\alpha}P_p + P_n) + \mathcal{P}(\mathcal{H}_0)w_iP_n) \quad (12)$$

where the symbol 'w_i' represents the power amplifier gain at SU_i. Due to the high computation, it is difficult to find the optimal w_i for an individual SU_i. Instead of calculating each SU's power gain, the separate power gain for each SU cluster is calculated. It is assumed that w_{ci} is the power gain of the ith cluster where $w_c = \sum_{i=1}^{c} w_{ci}$. The

E_{maxPU1}	876.19	775.78	922.98	548.01	780.98	823.34
	SU_1	SU_2	SU_1	SU_3	SU_1	SU_3
E_{maxPU2}	666.84	875.55	782.48	550.76	662.22	909.32
	SU_2	SU_1	SU_2	SU_2	SU_3	SU_1

Fig. 4. Energy set of E_{maxPU1}, E_{maxPU2}.

amplifying gain for the jth SU in the ith cluster is calculated as:

$$w_{c_{ij}} = \frac{d_{a_{ij}}}{\sum_{i=1}^{L} d_{a_{ij}}}$$

where the symbol '$d_{a_{ij}}$' represents the distance from the PU to the jth SU in the ith cluster. The optimal values of w_c and N are calculated using FCM and KFCM with differential evaluation (DE) technique [44]. The working procedure of the DE algorithm with FCM is described in [44]. In this work, the DE algorithm is applied to KFCM to find the optimal w_c and N values. The average energy consumption of all SUs is formulated as:

$$E_s = E_{BP} + E_{PA} + E_c. \tag{13}$$

Here E_{BP} represents the energy consumption in base-band processing circuits. The symbol E_{PA} represents the energy consumption due to the amplification at SU_i for forwarding the received signal to the FC. E_c represents the energy consumption for radio devices during the signal reception and transmission. E_{BP} and E_c values being much lower compared to E_{PA} are not considered in this experiment [44]. In all such cases, it is assumed as $E_s \approx E_{PA}$. The total energy consumption E_{PA} is written as:

$$E_{PA} = \sum_{i=1}^{K} P_i N T_{sa} \tag{14}$$

where T_{sa} represents the sampling interval and $T_{sense} = N \times T_{sa}$.

4. Numerical results and discussions

This section presents a large set of simulation results to highlight PU detection performance at low SNR, CSS performance gain over FCM [44] and analytical method [39], multiple PU detection results, energy consumption and sensing duration time required.

4.1. CSS at low SNR

Performance of the proposed KFCM based approach is compared with FCM [44] and the analytical technique proposed in [39] to highlight its relative improvement in CSS at low SNR. Monte Carlo simulations with 10,000 iterations are performed and the maximum energy values are stored in the E_{max} set during the 10,000 sensing slots (t_s).

Fig. 5 illustrates the receiver operating characteristics (ROC) curve which plots P_d against P_{fa} for the proposed three cluster based KFCM, four cluster based FCM [44] and the analytical approach [39]. For simulation purposes, the number of SUs is fixed to 10 and is partitioned into two clusters (SU_{c1} and SU_{c2}), depending on the respective distance from the PU. SU_{c1} and SU_{c2} cluster centers are assumed to be 1 m and 1.25 m, respectively, from the PU. In this case, the PU's transmission power is set at −10 dBW and noise variance (P_n) is fixed at 0 dBW, the sensing channels are considered to be Rayleigh distributed and the reporting channels are considered to be ideal, the number of samples (N) is fixed at 150, the path loss exponent of the channels are $\alpha_1 = 2$ for SU_{c1} and $\alpha_2 = 4$ for SU_{c2}. $\mathcal{P}(\mathcal{H}_1) = 0.30$ and $\mathcal{P}(\mathcal{H}_0) = 0.70$ represent the probabilities of the presence and the absence of PU's in CRN.

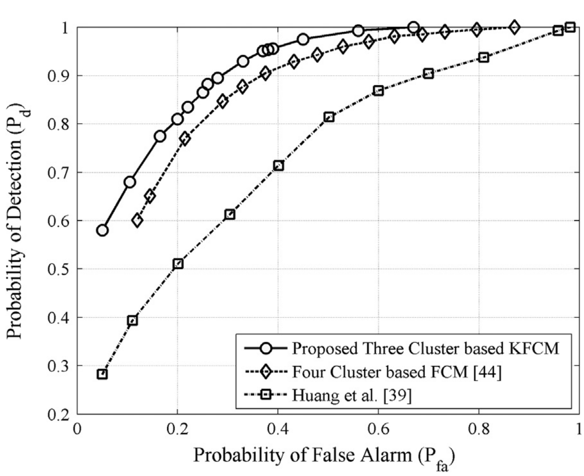

Fig. 5. Receiver operating characteristic curves (P_d vs. P_{fa}).

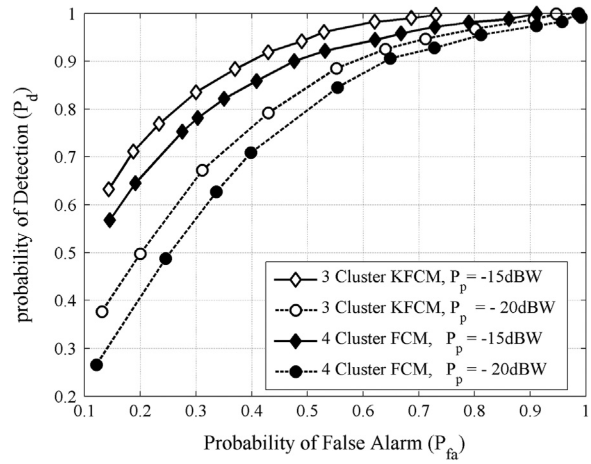

Fig. 6. Receiver operating characteristic curves (P_d vs. P_{fa}).

The graphical results show that the three cluster based KFCM offers improved results over both the four clusters based FCM algorithm [44] and analytical approach [39]. From Fig. 5, it is also observed that the proposed KFCM method offers a P_d value above 0.9 at P_{fa}=0.3, while P_d valuing for [44] and [39] are 0.82 and 0.60, respectively, at the same P_{fa} and at a low PU power of −10 dBW. The three cluster based KFCM improves the detection probability (P_d) by ~6.56% over the four cluster based FCM [44] at $P_{fa} = 0.12$. It is observed that a gain in P_d value by ~80% for the three cluster based KFCM over [39] is achieved when $P_{fa} = 0.12$.

Fig. 6 illustrates the ROC curve which plots P_d against P_{fa} of KFCM and FCM. In this case, the PU transmit power are considered: −15 dBW and −20 dBW for two different cases, the number of samples (N) is fixed at 1000, and the other parameter values are the same as in the previous case. An improvement in P_d value for the three cluster based KFCM over the four cluster based FCM [44] is clearly observed in Fig. 6. From Fig. 6, the KFCM improves detection performance over FCM [44] by ~6.78% and ~6.96% at −15 dBW and −20 dBW, respectively, when $P_{fa} = 0.14$.

Fig. 7 shows the performance comparison with [44,39] for P_d vs. the number of samples (equivalent to the sensing duration). The graphical results show that the three cluster based KFCM offers significant performance gain over the four cluster based FCM [44,39] at low sample values. The PU power is fixed at −10 dBW and the number of samples (N) increases from 100 to 1000. From Fig. 7, it is clearly observed that the P_d value increases with the increase in the number of samples (N). As the N value increases from 100 to 1000, about ~24.67% gain in the P_d value is noted for the three cluster based KFCM. It is also observed that the three cluster based KFCM provides improved performance in the P_d value over the four cluster based FCM [44] at a smaller number of samples (N). A gain in the P_d value by ~6.78% is noted for the three cluster based KFCM compared to the four cluster based FCM [44] when N=100. The KFCM results are also compared to the technique proposed in [39]. A gain in the P_d value by ~56% for the three cluster based KFCM is noted over the technique proposed in [39] when N=100. The P_d values for the proposed method are above 0.90 at N=400.

Fig. 8 shows the performance comparison with [44,39] for the

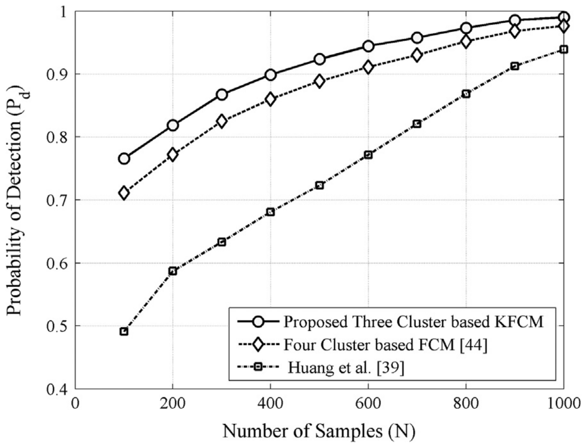

Fig. 7. Probability of detection P_d vs. number of samples (N).

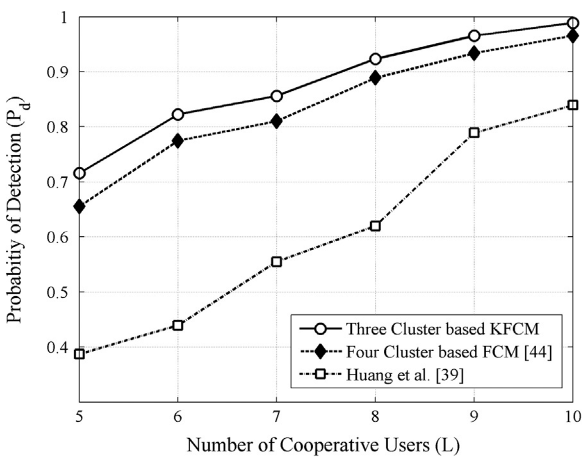

Fig. 8. Probability of detection P_d vs. number of cooperative users (L).

changes in P_d when the number of cooperative users (L) varies. In this case, the PU transmit signal power (P_p) is fixed at −10 dBW, the number of SUs (L) varies from 5% to 10%, and the rest of the parameters are set the same as previous cases. The graphical results show that the proposed three cluster based KFCM improves the detection performance from 0.71 to 0.98 as the L value is increased from 5 to 10. The graphical results also show about a ~22.04% gain in the P_d value for the three cluster based KFCM is achieved when the L value is increased from 5 to 10. It is also observed that the three cluster based KFCM performs better than the existing methods [44,39] when the number of relays (L) is less. A gain in the P_d value by ~6.28% is noted for the proposed method compared to the four cluster based FCM [44] and a gain in the P_d value by ~73.17% for the proposed method is observed over the analytical approach [39] when L=5. It is observed that the P_d values for the proposed method are above 0.9 for L=8.

Fig. 9 shows the variation of P_d with the transmission power of PU (P_p). The graphical results show that the three cluster based KFCM performs better than the four cluster based FCM [44] when the PU transmit power is decreased. The number of samples N is set at 1000 and the L value is fixed at 10. From Fig. 9, it is clearly observed that KFCM improves the detection rate (P_d) by ~2.97% and ~16.32% at $P_p = -20$ dBW over the FCM based CSS scheme [44] and the proposed technique in [39]. Simulation results thus show that KFCM is found to be more efficient than FCM [44] and the analytical approach [39] at low SNR with high P_d values.

4.2. Multiple PU detection

This subsection presents the simulation results of multiple PU

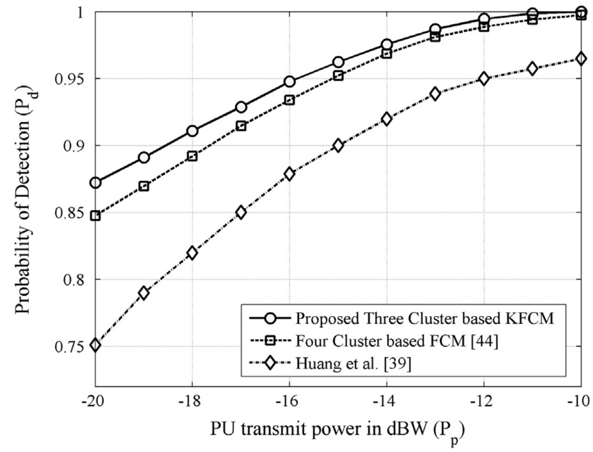

Fig. 9. P_d vs. PU transmit power.

detection performance of the proposed technique. Monte Carlo simulations with 10,000 iterations are performed to store the maximum energy values for the individual PU at the FC. Here, $\mathcal{P}(\mathcal{H}_1) = 0.30$ and $\mathcal{P}(\mathcal{H}_0) = 0.70$ represent the probability of active and ideal state of the PU, respectively.

Fig. 10 represents the performance of the three cluster based KFCM and Fig. 11 represents the performance of the four cluster based FCM for multiple PU detection. The performance comparison in both the cases is represented by an ROC curve that shows the variation in detection probability (P_d) vs. false alarm probability (P_{fa}). Simulation parameters are considered to be the same for Figs. 10 and 11. The parameters are as follows: the total number of PUs is set to 4, the total number of SUs is fixed to 30, the path loss exponent α is chosen randomly between 2 and 4, the P_n value is set to 0 dBW and the number of samples is fixed at 2000, the P_p values are taken as −15 dBW,−15.5 dBW,−16 dBW and −16.5 dBW for PU_1, PU_2, PU_3 and PU_4, respectively.

From Figs. 10 and 11, it is clearly observed that the proposed scheme of SU clustering works well to detect multiple PUs. From Figs. 10 and 11, it is observed that KFCM gives a higher detection rate for all PUs compared to the FCM based technique. It is observed from Fig. 10 that before SU clustering, KFCM yields the P_d value 0.9 when p_{fa} is 0.3 for PU_1 and after SU clustering, KFCM shows the P_d value 0.89 at p_{fa}=0.3 for PU_1. Fig. 11 shows that before SU clustering, FCM offers the P_d value 0.86 when p_{fa} is 0.3 for PU_1 and after SU clustering, FCM yields the P_d value 0.85 at p_{fa}=0.3 for PU_1. The graphical results show that KFCM improves the detection performance by ~4.65% and ~3.37% before and after SU clustering over FCM for PU_1 when p_{fa}=0.3.

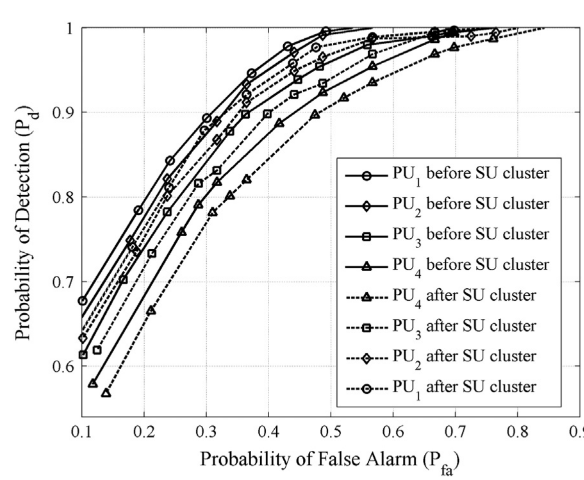

Fig. 10. Receiver operating characteristic curves (P_d vs. P_{fa}) using KFCM.

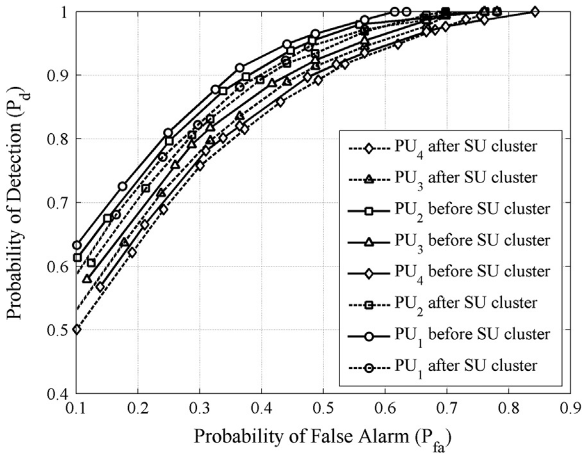

Fig. 11. Receiver operating characteristic curves (P_d vs. P_{fa}) using FCM.

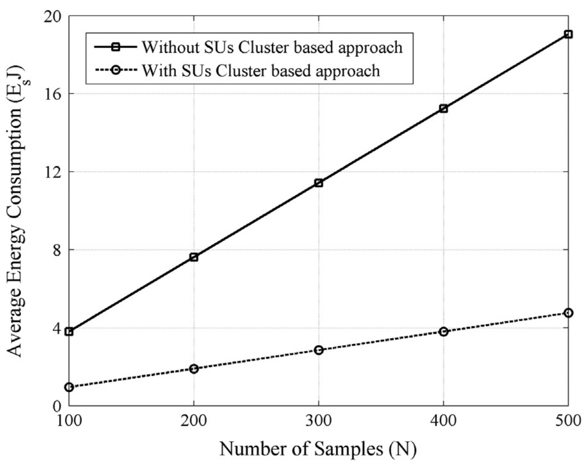

Fig. 12. Average energy consumption E_s vs. number of samples.

The same comparison between KFCM and FCM is done for PU_2, PU_3, PU_4. It is found that, for each one of these PU detection scenarios, KFCM offers better results than FCM. From the results, it is observed that P_d values fall slightly (~1.11% in KFCM) when an individual of a SU cluster senses a particular PU compared to the case when all SUs participate to sense a particular PU. However, the total energy consumption is reduced significantly for the SUs cluster based approach over the latter method. From Fig. 12, it is clearly observed that the average energy consumption is significantly reduced by the cluster based approach of SUs. The w_c value is fixed at 11.5 and $N = \{100, \ldots 500\}$%, the average distance between a SU to PU is fixed at 1.25 m, in this case. From Fig. 12, about ~75.02% saving in average energy consumption is observed for the SUs clustering than the non-cluster based approach at N=100.

4.3. Energy efficient CSS using KFCM clustering

The relative improvement in energy efficiency using the proposed technique over the optimal FCM [40] and the technique proposed in [39] is shown in Fig. 13. In this case, the average distance between the PU and an SU is set at 1 m and the distance between the FC to SU is fixed at 2 m. The set of simulation parameters is as follows: $N = \{50, \ldots 1000\}$, $w_c = \{2, \ldots 100\}$, α=4, $P(\mathcal{H}_1) = 0.30$ and $\mathcal{P}(\mathcal{H}_0) = 0.70$, P_n=0 dBW, P_p=0 dBW, L=10, T_{sa}=1 ms. The symbol 'T_{sa}' represents the sampling interval. The optimal w_i and N values are calculated through the differential evolution (DE) algorithm for each FCM and KFCM.

Fig. 13 shows the variation of the average energy consumption of

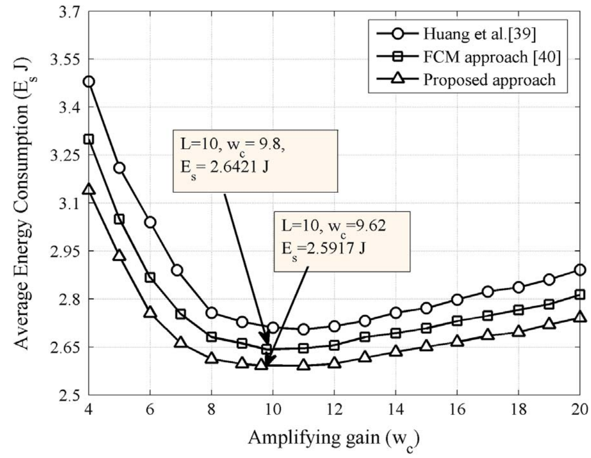

Fig. 13. Average SU energy consumption E_s vs. total SU amplifying gain w_c.

the SUs with the amplifying gain w_c. For both FCM and KFCM, it is observed that E_s decreases with an initial increase in w_c. The proposed KFCM approach is compared with the optimal FCM [40] and the technique proposed in [39]. FCM-DE provides the optimum values for w_c and N as 9.8 and 64, respectively, to meet the target $P_d \geq 0.90$ and $p_{fa} \leq 0.05$. On the other hand, KFCM-DE provides the optimum values for w_c and N as 9.62 and 58, respectively. Thus, not only an improved performance in energy consumption is achieved but also a gain in sensing duration is achieved. The performance results are shown in Fig. 14 where a variation in the average energy consumption vs. number of samples is shown. The number of samples can be considered as the sensing duration. Since SS is done periodically on a frame by frame basis, the low sensing duration requirement offers one way the longer duration for SU transmission. Hence the proposed CSS scheme is not only energy efficient but also fast and reliable enough. Furthermore, there is a consequent gain in SU throughput when the proposed CSS model is applied to joint SS and SU transmission. It is observed from the Fig. 14 that the KFCM algorithm improves the energy consumption (E_s) minimization by ~1.18% over FCM [40], and ~4.36% over the technique proposed in [39]. It is also noted from Fig. 14 that KFCM gives the optimal energy consumption while meeting $P_d \geq 0.90$ and $p_{fa} \leq 0.05$ at less samples (N=58).

5. Conclusions and scope of future works

The proposed work shows the efficacy of KFCM over FCM on an energy detection based CSS scheme at low SNR and multiple PU detection. For a single PU, it is observed that the proposed KFCM method offers detection probability value above 0.9 at false alarm

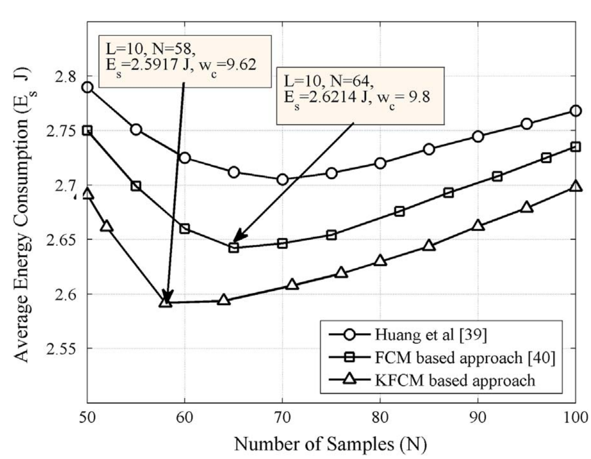

Fig. 14. Average SU energy consumption E_s vs. the number of samples N.

probability 0.3 when PU power is at −10 dBW. It is also observed that the KFCM based CSS offers a higher detection probability when the number of relays (L) and the number of samples (N) are relatively less compared to the existing FCM based and analytic methods. For multiple PU detection, it is observed that the KFCM based method offers, on average, ~0.86 individual detection probability at a very low PU power ~−16 dB and it is also noted that average energy consumption is reduced by ~75.02% through SUs clustering. The proposed KFCM based CSS is not only energy efficient but also provides faster sensing compared to optimal FCM which in turn increases the data transmission duration. The KFCM algorithm improves the energy consumption (E_s) minimization by ~1.18% over the optimal FCM, while meeting the same detection probability ~0.90 and false alarm probability ~0.05.

Some of the future works may be as follows:

- The proposed work may be extended in the joint SS and data transmission framework to evaluate the gain in energy minimization and throughput improvement over the FCM based method.
- Similar to [40], the proposed work may be extended as an energy minimization problem under the constraints of detection reliability for an individual PU.

References

[1] Federal Communications Commission, Spectrum policy task force, Report ET Docket No. 02-135, 2002.
[2] OFCOM, Digital Dividend Review, A Statement on Our Approach Towards Awarding the Digital Dividend, 2007.
[3] J. Mitola, Cognitive radio: an integrated agent architecture for software defined radio (Ph.D. dissertation), Computer Communication System Laboratory, Department of Teleinformatics, Royal Institute of Technology (KTH), Stockholm, Sweden, May 2000.
[4] Y. Zou, Y.-D. Yao, B. Zheng, Cognitive transmissions with multiple relays in cognitive radio networks, IEEE Trans. Wirel. Commun. 10 (2) (2011) 648–659.
[5] S. Haykin, Cognitive radio: brain-empowered wireless communications, IEEE J. Sel. Areas Commun. 23 (2) (2005) 201–220.
[6] M. Masonta, M. Mzyece, N. Ntlatlapa, Spectrum decision in cognitive radio networks: a survey, IEEE Commun. Surv. Tutor. 15 (3) (2013) 1088–1107.
[7] I.F. Akyildiz, B.F. Lo, R. Balakrishnan, Cooperative spectrum sensing in cognitive radio networks: a survey, Phys. Commun. 4 (1) (2011) 40–62.
[8] M. Feng, T. Jiang, D. Chen, S. Mao, Cooperative small cell networks: high capacity for hotspots with interference mitigation, IEEE Wirel. Commun. 21 (December) (2014) 108–116.
[9] C.H. Lee, W. Wolf, Multiple access-inspired cooperative spectrum sensing for cognitive radio, in: Proceedings of IEEE Military Communications Conference (MILCOM), 2007, pp. 1–6.
[10] C. Sun, W. Zhang, K. Ben, Cluster-based cooperative spectrum sensing in cognitive radio systems, in: Proceedings IEEE International Conference on Communications (ICC), 2007, pp. 2511–2515.
[11] I. Sobron, P. Diniz, W. Martins, M. Velez, Energy detection technique for adaptive spectrum sensing, IEEE Trans. Commun. 63 (3) (2015) 617–627.
[12] Y. Mingchuan, L. Yuan, L. Xiaofeng, T. Wenyan, Cyclostationary feature detection based spectrum sensing algorithm under complicated electromagnetic environment in cognitive radio networks, China Commun. 12 (9) (2015) 35–44.
[13] Y. Zeng, Y.-C. Liang, Eigenvalue-based spectrum sensing algorithms for cognitive radio, IEEE Trans. Commun. 57 (6) (2009) 1784–1793.
[14] W. Sun, Z. Huang, F. Wang, X. Wang, Compressive wideband spectrum sensing based on single channel, Electron. Lett. 51 (9) (2015) 693–695.
[15] Z. Xinzhi, G. Feifei, C. Rong, J. Tao, Matched filter based spectrum sensing when primary user has multiple power levels, China Commun. 12 (2) (2015) 21–31.
[16] S. Sedighi, A. Taherpour, S. Monfared, Bayesian generalised likelihood ratio test-based multiple antenna spectrum sensing for cognitive radios, IET Commun. 7 (18) (2013) 2151–2165.
[17] Y. Zhang, Q. Zhang, S. Wu, Entropy-based robust spectrum sensing in cognitive radio, IET Commun. 4 (4) (2010) 428–436.
[18] Y.L. Xu, H.S. Zhang, Z.H. Han, The performance analysis of spectrum sensing algorithms based on wavelet edge detection, in: Proceedings of 5th International Conference on Wireless Communications, Networking and Mobile Computing (WiCom), 2009, pp. 1–4.
[19] J. Shen, T. Jiang, S. Liu, Z. Zhang, Maximum channel throughput via cooperative spectrum sensing in cognitive radio networks, IEEE Trans. Wirel. Commun. 8 (October) (2009) 5166–5175.
[20] R.R. Jaglan, S. Sarowa, R. Mustafa, S. Agrawal, N. Kumar, Comparative study of single-user spectrum sensing techniques in cognitive radio networks, Proc. Comput. Sci. 58 (2015) 121–128.
[21] T. Yucek, H. Arslan, A survey of spectrum sensing algorithms for cognitive radio applications, IEEE Commun. Surv. Tutor. 11 (1) (2009) 116–130.
[22] D. Bhargavi, C. Murthy, Performance comparison of energy, matched-filter and cyclostationarity-based spectrum sensing, in: Proceedings of IEEE Eleventh International Workshop on Signal Processing Advances in Wireless Communications (SPAWC), 2010, pp. 1–5.
[23] P. Sutton, K. Nolan, L. Doyle, Cyclostationary signatures in practical cognitive radio applications, IEEE J. Sel. Areas Commun. 26 (January) (2008) 13–24.
[24] E. Rebeiz, P. Urriza, D. Cabric, Optimizing wideband cyclostationary spectrum sensing under receiver impairments, IEEE Trans. Signal Process. 61 (August) (2013) 3931–3943.
[25] A. Sonnenschein, P. Fishman, Radiometric detection of spread-spectrum signals in noise of uncertain power, IEEE Trans. Aerosp. Electron. Syst. 28 (July) (1992) 654–660.
[26] V. Sharma, V. Bohara, Exploiting machine learning algorithms for cognitive radio, in: Proceedings of International Conference on Advances in Computing, Communications and Informatics (ICACCI), 2014, pp. 1554–1558.
[27] M. Bkassiny, Y. Li, S. Jayaweera, A survey on machine-learning techniques in cognitive radios, IEEE Commun. Surveys Tutor. 15 (3) (2013) 1136–1159.
[28] K. Thilina, K.W. Choi, N. Saquib, E. Hossain, Machine learning techniques for cooperative spectrum sensing in cognitive radio networks, IEEE J. Sel. Areas Commun. 31 (November) (2013) 2209–2221.
[29] C. Clancy, J. Hecker, E. Stuntebeck, T. O'Shea, Applications of machine learning to cognitive radio networks, IEEE Wirel. Commun. 14 (August) (2007) 47–52.
[30] X.L. Huang, F. Hu, J. Wu, H.H. Chen, G. Wang, T. Jiang, Intelligent cooperative spectrum sensing via hierarchical Dirichlet process in cognitive radio networks, IEEE J. Sel. Areas Commun. 33 (May) (2015) 771–787.
[31] M. Bkassiny, S. Jayaweera, Y. Li, K. Avery, Wideband spectrum sensing and non-parametric signal classification for autonomous self-learning cognitive radios, IEEE Trans. Wirel. Commun. 11 (July) (2012) 2596–2605.
[32] S. Gong, W. Liu, W. Yuan, W. Cheng, S. Wang, Threshold-learning in local spectrum sensing of cognitive radio, in: Proceedings of IEEE 69th Vehicular Technology Conference (VTC), 2009, pp. 1–6.
[33] R. Rashid, A. Bin Abdul Hamid, N. Fisal, S. Syed-Yusof, H. Hosseini, A. Lo, A. Farzamnia, Efficient in-band spectrum sensing using swarm intelligence for cognitive radio network, Can. J. Electr. Comput. Eng. 38 (2) (2015) 106–115.
[34] A. Ghasemi, E.S. Sousa, Collaborative spectrum sensing for opportunistic access in fading environments, in: Proceedings of First IEEE International Symposium on New Frontiers in Dynamic Spectrum Access Networks (DySPAN), 2005, pp. 131–136.
[35] E. Visotsky, S. Kuffner, R. Peterson, On collaborative detection of tv transmissions in support of dynamic spectrum sharing, in: Proceedings of First IEEE International Symposium on New Frontiers in Dynamic Spectrum Access Networks (DySPAN), 2005, pp. 338–345.
[36] T. Newman, R. Rajbanshi, A.M. Wyglinski, J. Evans, G. Minden, Population adaptation for genetic algorithm-based cognitive radios, in: Proceedings of 2nd International Conference on Cognitive Radio Oriented Wireless Networks and Communications (CrownCom), 2007, pp. 279–284.
[37] M. Sanna, M. Murroni, Optimization of non-convex multiband cooperative sensing with genetic algorithms, IEEE J. Sel. Top. Signal Process. 5 (February) (2011) 87–96.
[38] Z. Zhao, Z. Peng, S. Zheng, J. Shang, Cognitive radio spectrum allocation using evolutionary algorithms, IEEE Trans. Wirel. Commun. 8 (September) (2009) 4421–4425.
[39] S. Huang, H. Chen, Y. Zhang, F. Zhao, Energy-efficient cooperative spectrum sensing with amplify-and-forward relaying, IEEE Commun. Lett. 16 (April) (2012) 450–453.
[40] S.P. Maity, S. Chatterjee, T. Acharya, On optimal fuzzy c-means clustering for energy efficient cooperative spectrum sensing in cognitive radio networks, Digit. Signal Process. 49 (February) (2016) 104–115.
[41] F. Yu, M. Huang, H. Tang, Biologically inspired consensus-based spectrum sensing in mobile ad hoc networks with cognitive radios, IEEE Netw. 24 (May) (2010) 26–30.
[42] N. Reisi, M. Ahmadian, V. Jamali, S. Salari, Cluster-based cooperative spectrum sensing over correlated log-normal channels with noise uncertainty in cognitive radio networks, IET Commun. 6 (November) (2012) 2725–2733.
[43] G. Caso, H. Soleimani, L. De Nardis, A. Tosti, M. Di Benedetto, Sensic: mobility-aware cluster-based cooperative spectrum sensing for cognitive radio networks, in: Proceedings of IEEE International Conference on Ultra-WideBand (ICUWB), 2014, pp. 102–107.
[44] S. Chatterjee, A. Banerjee, T. Acharya, S.P. Maity, Fuzzy c-means clustering in energy detection for cooperative spectrum sensing in cognitive radio system, in: Proceedings of Multiple Access Communications (MACOM), vol. 8715, 2014, pp. 84–95.
[45] G. Huang, S. Song, J.N.D. Gupta, C. Wu, Semi-supervised and unsupervised extreme learning machines, IEEE Trans. Cybern. 44 (December) (2014) 2405–2417.
[46] M.W. Libbrecht, W.S. Noble, Machine learning applications in genetics and genomics, Nat. Rev. Genet. 16 (June) (2015) 321–332.
[47] M.A. Alsheikh, S. Lin, D. Niyato, H.P. Tan, Machine learning in wireless sensor networks: algorithms, strategies, and applications, IEEE Commun. Surv. Tutor. 16 (4) (2014) 1996–2018.
[48] Z. Bai, L. Wang, H. Zhang, K. Kwak, Cluster-based cooperative spectrum sensing for cognitive radio under bandwidth constraints, in: Proceedings of IEEE International Conference on Communication Systems (ICCS), 2010, pp. 569–573.
[49] A. Kozal, M. Merabti, F. Bouhafs, Spectrum sensing-energy tradeoff in multi-hop cluster based cooperative cognitive radio networks, in: Proceedings of IEEE Conference on Computer Communications Workshops (INFOCOM WKSHPS),

2014, pp. 765–770.
[50] L. Wang, J. Wang, G. Ding, F. Song, Q. Wu, A survey of cluster-based cooperative spectrum sensing in cognitive radio networks, in: Proceedings of Cross Strait Quad-Regional Radio Science and Wireless Technology Conference (CSQRWC), vol. 1, 2011, pp. 247–251.
[51] T. Dhope, D. Simunic, Cluster based cooperative sensing:-a survey, in: Proceedings of International Conference on Communication, Information Computing Technology (ICCICT), 2012, pp. 1–6.
[52] Z. dong Wu, W. xin Xie, J. ping Yu, Fuzzy c-means clustering algorithm based on kernel method, in: Proceedings of Fifth International Conference on Computational Intelligence and Multimedia Applications (ICCIMA), 2003, pp. 49–54.
[53] M. Girolami, Mercer kernel-based clustering in feature space, IEEE Trans. Neural Netw. 13 (May) (2002) 780–784.
[54] D. Graves, W. Pedrycz, Kernel-based fuzzy clustering and fuzzy clustering: a comparative experimental study, Fuzzy Sets Syst. 161 (4) (2010) 522–543.
[55] B. Chen, T. Liu, F. Shu, J. Wang, On performance comparison of wideband multiple primary user detection methods in cognitive radios, in: Proceedings of 5th International Conference on Wireless Communications, Networking and Mobile Computing (WiCom), September 2009, pp. 1–4.
[56] R. Louie, M. McKay, Y. Chen, Multiple-antenna signal detection in cognitive radio networks with multiple primary user signals, in: Proceedings of IEEE International Conference on Communications (ICC), 2014, pp. 4951–4956.
[57] D. Morales-Jimenez, R. Louie, M. McKay, Y. Chen, Analysis and design of multiple-antenna cognitive radios with multiple primary user signals, IEEE Trans. Signal Process. 63 (September) (2015) 4925–4939.
[58] L. Wei, O. Tirkkonen, Spectrum sensing in the presence of multiple primary users, IEEE Trans. Commun. 60 (May) (2012) 1268–1277.